

Supplementary Information

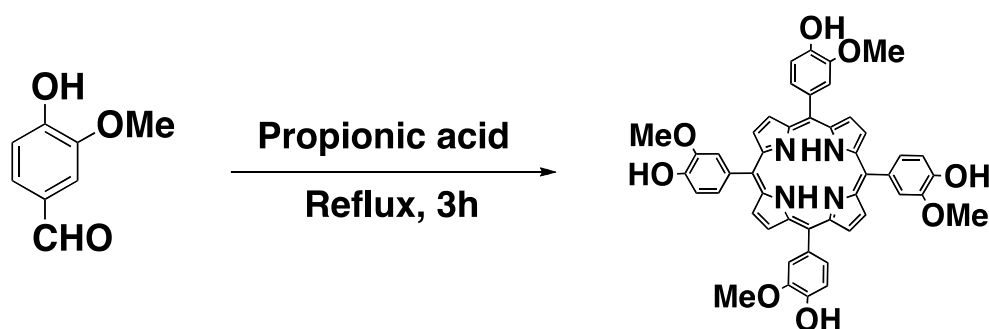
Supercapacitive hybrid materials from the thermolysis of porous coordination nanorods based on a catechol porphyrin

Shangbin Jin, Jonathan P. Hill, Qingmin Ji, Lok Kumar Shrestha and Katsuhiko Ariga

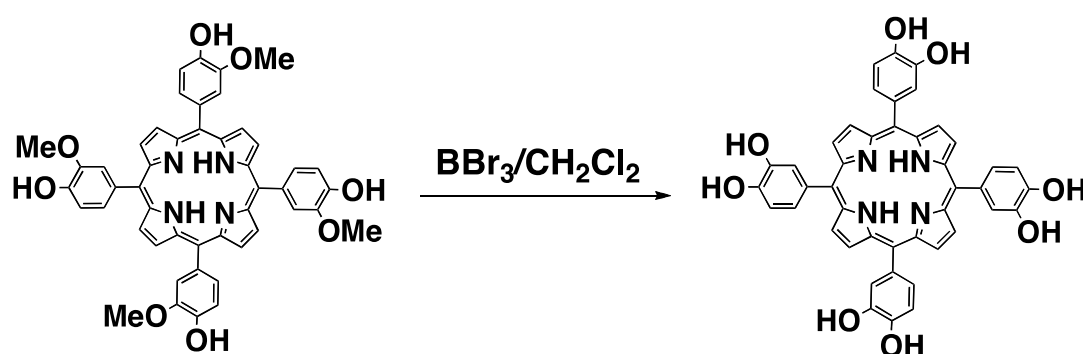
CONTENTS:

1.0 Synthesis of catechol porphyrin	S2
2.0 Additional Figures	
Figure S1. ¹ H NMR of <i>meso</i> -tetrakis(3,4-dihydroxyphenyl)porphyrin	S4
Figure S2. Powder X-ray diffraction profiles of MCP-PCPs	S4
Figure S3 – S5. Nitrogen sorption curves	S5
Figure S6. FE-SEM images	S6
Figure S7. HR-TEM images	S7
Figure S8. XPS survey scans for MCP-PCP@800	S8
Figure S9. XPS spectra for MCP-PCP@800	S9
Figure S10. Specific capacitance vs current density for MCP-PCP@800	S10
Figure S11. Cyclic stability test by charge-discharge measurements	S11
Figure S12. Charge-discharge curves at 2 A/g showing 1 st and 2 nd cycles	S12
3.0 References	S13

1.0 Synthesis of catechol porphyrin ligand



Meso-tetrakis(3-methoxy-4-hydroxyphenyl)porphyrin^{S1,S2} Vanillin (15.2 g, 0.1 mol) was dissolved in propionic acid (500 mL) and heated to 150 °C. Pyrrole (6.7 g, 0.1 mol) was added dropwise to the resulting solution. The solution was then refluxed for 3 h under air then cooled to room temperature followed by distillation of propionic acid under reduced pressure to a volume of approx. 200 mL and the resulting dark solution was allowed to stand under ambient conditions overnight. The precipitate that formed was collected by filtration, washed with methanol and dried under reduced pressure overnight yielding a purple powder (2.6 g, 13 % yield). ¹H-NMR (300 MHz, DMSO-*d*₆): 9.52 (s, 4H), 8.91 (s, 8H), 7.77 (s, 4H), 7.58 (d, 4H), 7.21 (d, 4H), 3.89 (s, 12 H), -2.87(s, 2H). MALDI-TOF-MS (dithranol): found: 798.84, calcd: C₄₈H₃₈N₄O₈ 798.27 ([M⁺]).



Meso-tetrakis(3,4-dihydroxyphenyl)porphyrin.^{S2} A 50 mL two-neck flask was charged with *meso*-tetrakis(3-methoxy-4-hydroxyphenyl)porphyrin (0.8 g, 1 mmol) and dehydrated dichloromethane (10 mL) was added giving a clear red-purple solution which was cooled to 0 °C. Boron tribromide (7 mL, 1M in CH₂Cl₂) was added to the solution stirring continued at

room temperature for 72 h. The reaction mixture was then cooled to 0 °C and methanol (10 mL) was added followed by stirring for 30 min. The precipitate that formed was collected by filtration and washed with deionized water and methanol. The product was further purified by flash column chromatography on silica eluting with tetrahydrofuran. Product containing fractions were combined and solvents removed under reduced pressure yielding the product as purple powder. (Yield: 70 % yield). ¹H-NMR (see below, 300 MHz, *d*₆-acetone): 8.97 (bs, 8H), 8.32 (s, 8H), 7.74 (d, *J* = 2.1 Hz, 4H), 7.58 (dd, *J* = 2.1 Hz, 4.8 Hz, 4H), 7.55 (d, *J* = 4.8Hz, 4H), -2.70 (s, 2H). MALDI-TOF-MS (dithranol): found 746.53, calculated: C₄₄H₃₁N₄O₈ 746.22 ([M+H⁺]).

2.0 Additional Figures.

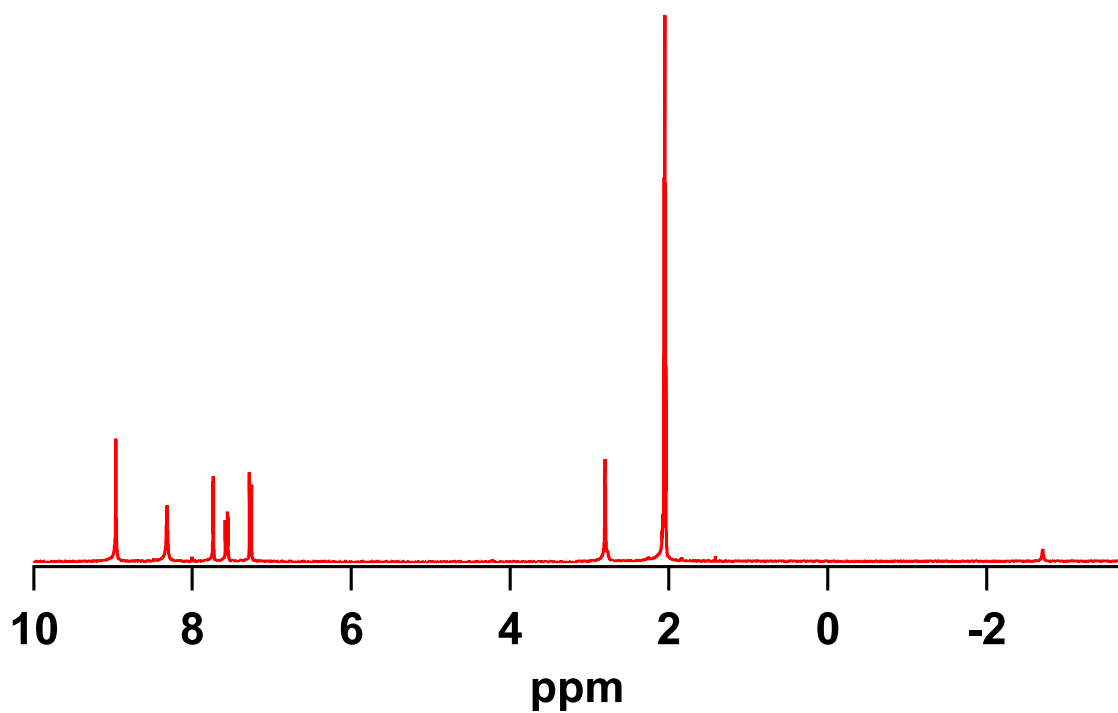


Figure S1. ¹H NMR of *meso*-tetrakis(3,4-dihydroxyphenyl)porphyrin in *d*₆-acetone.

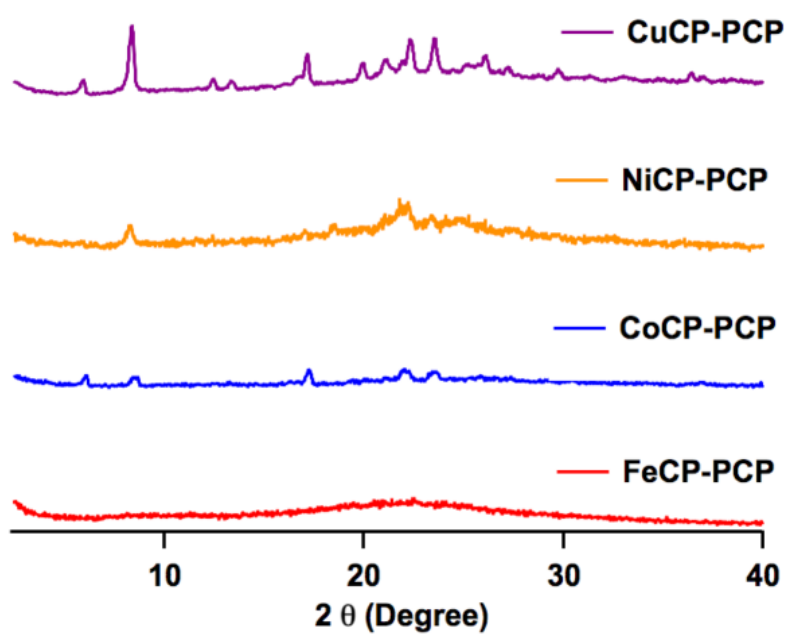


Figure S2. Powder X-ray diffraction profiles of MCP-PCPs.

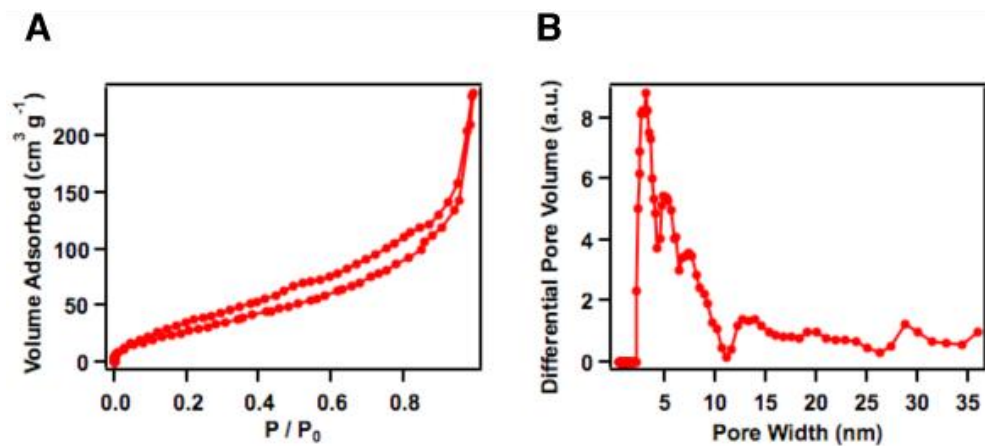


Figure S3. Nitrogen sorption isotherm curve (A) and pore size distribution (B) of FeCP-PCP at 77K.

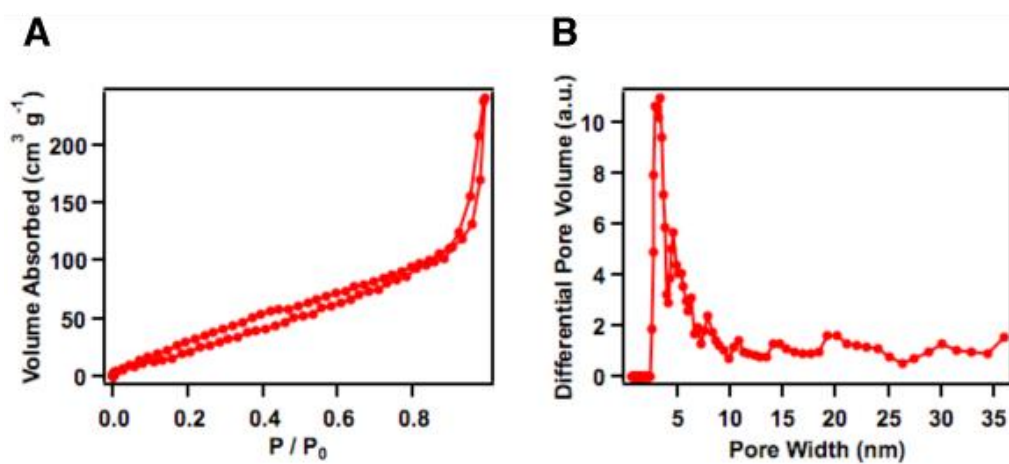


Figure S4. Nitrogen sorption isotherm curve (A) and pore size distribution (B) of CoCP-PCP at 77K.

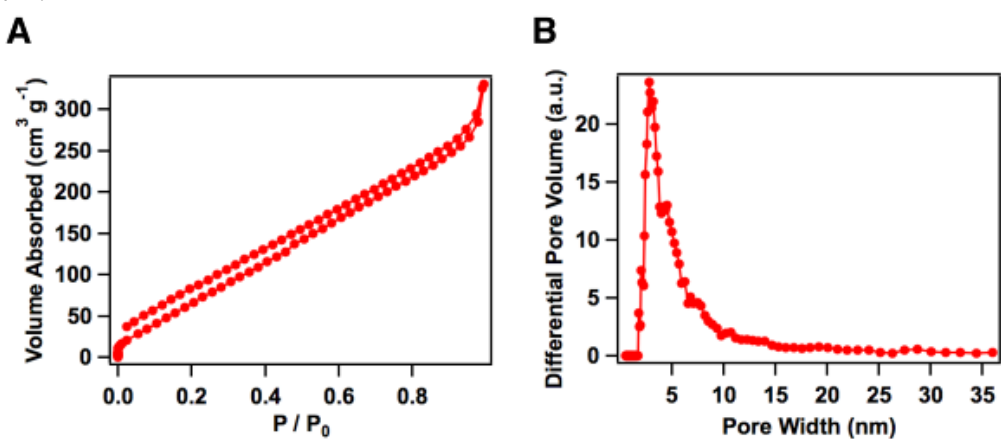


Figure S5. Nitrogen sorption isotherm curve (A) and pore size distribution (B) of NiCP-PCP at 77K.

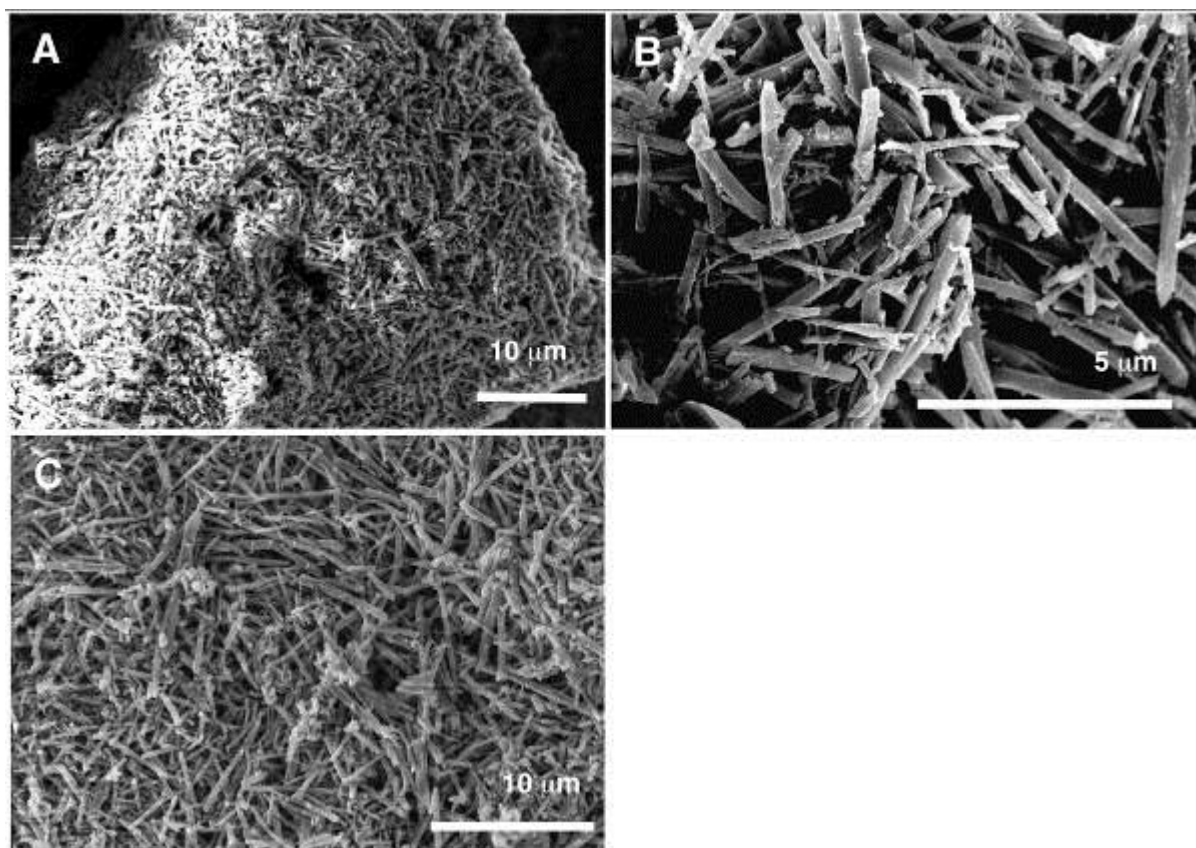


Figure S6. FE-SEM images of (A) FeCP-PCP, (B) CoCP-PCP, (C) NiCP-PCP.

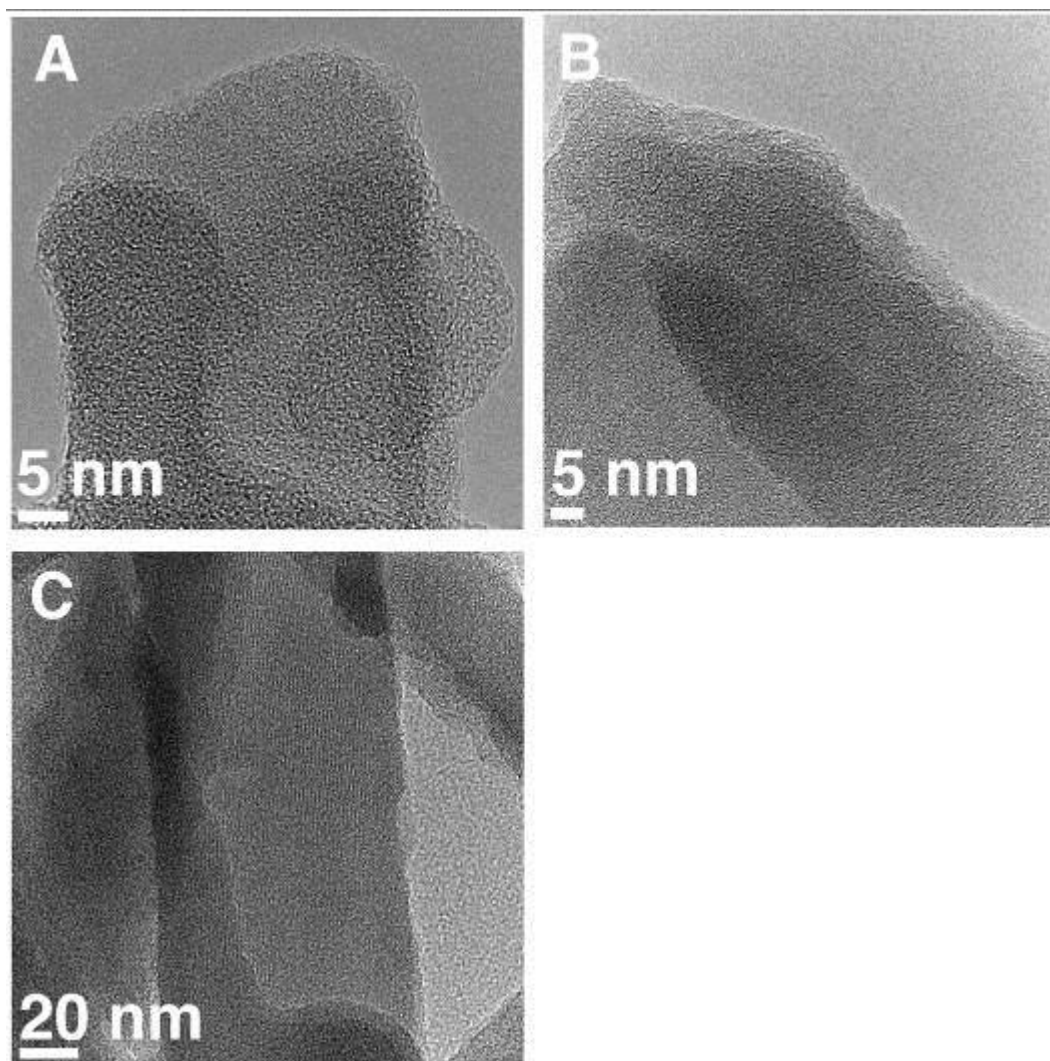


Figure S7. HR-TEM images of (A) FeCP-PCP, (B) CoCP-PCP, (C) NiCP-PCP.

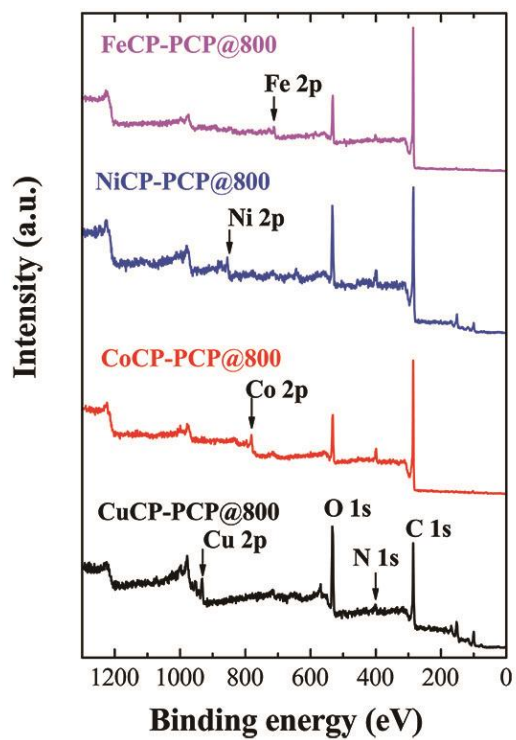


Figure S8. XPS survey scans for MCP-PCP@800 (metal as indicated in figure).

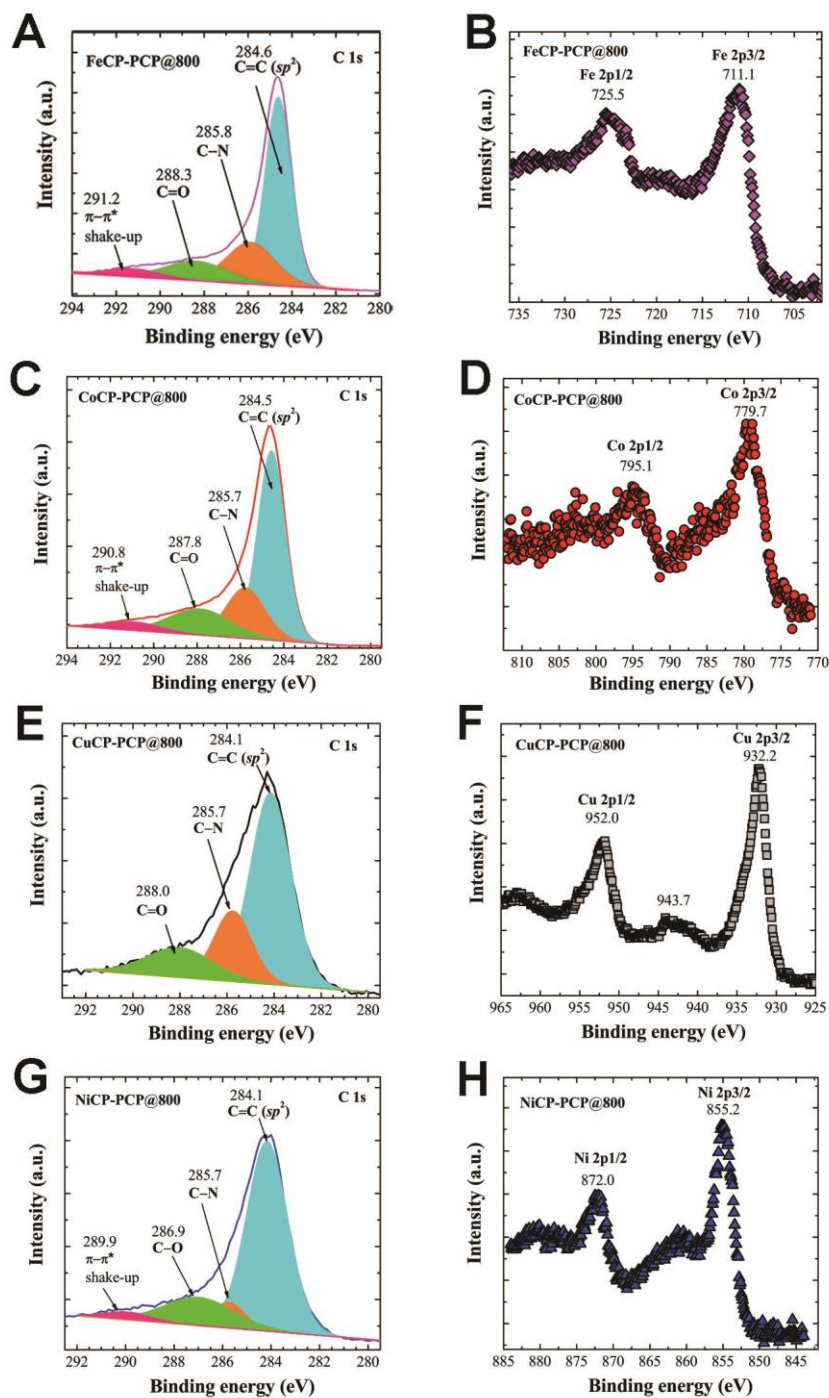


Figure S9. XPS spectra for MCP-PCP@800. FeCP-PCP@800: (A) C 1s (B) Fe 2p. CoCP-PCP@800: (C) C 1s (D) Co 2p. CuCP-PCP@800: (E) C 1s (F) Cu 2p. NiCP-PCP@800: (G) C 1s (H) Ni 2p.

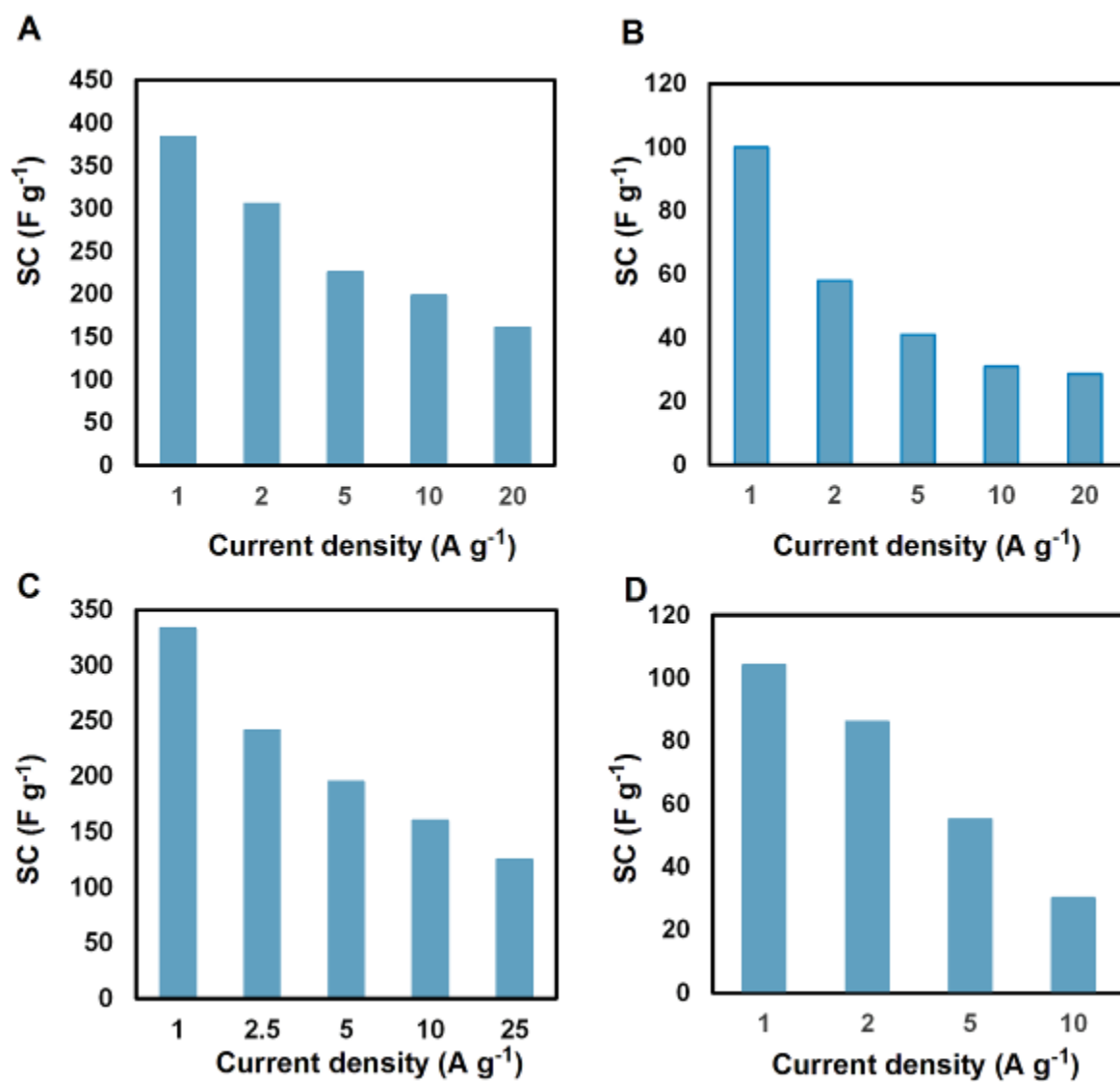


Figure S10. Specific capacitance vs current density for (A) FeCP-PCP@800, (B) CoCP-PCP@800, (C) NiCP-PCP@800, (D) CuCP-PCP@800.

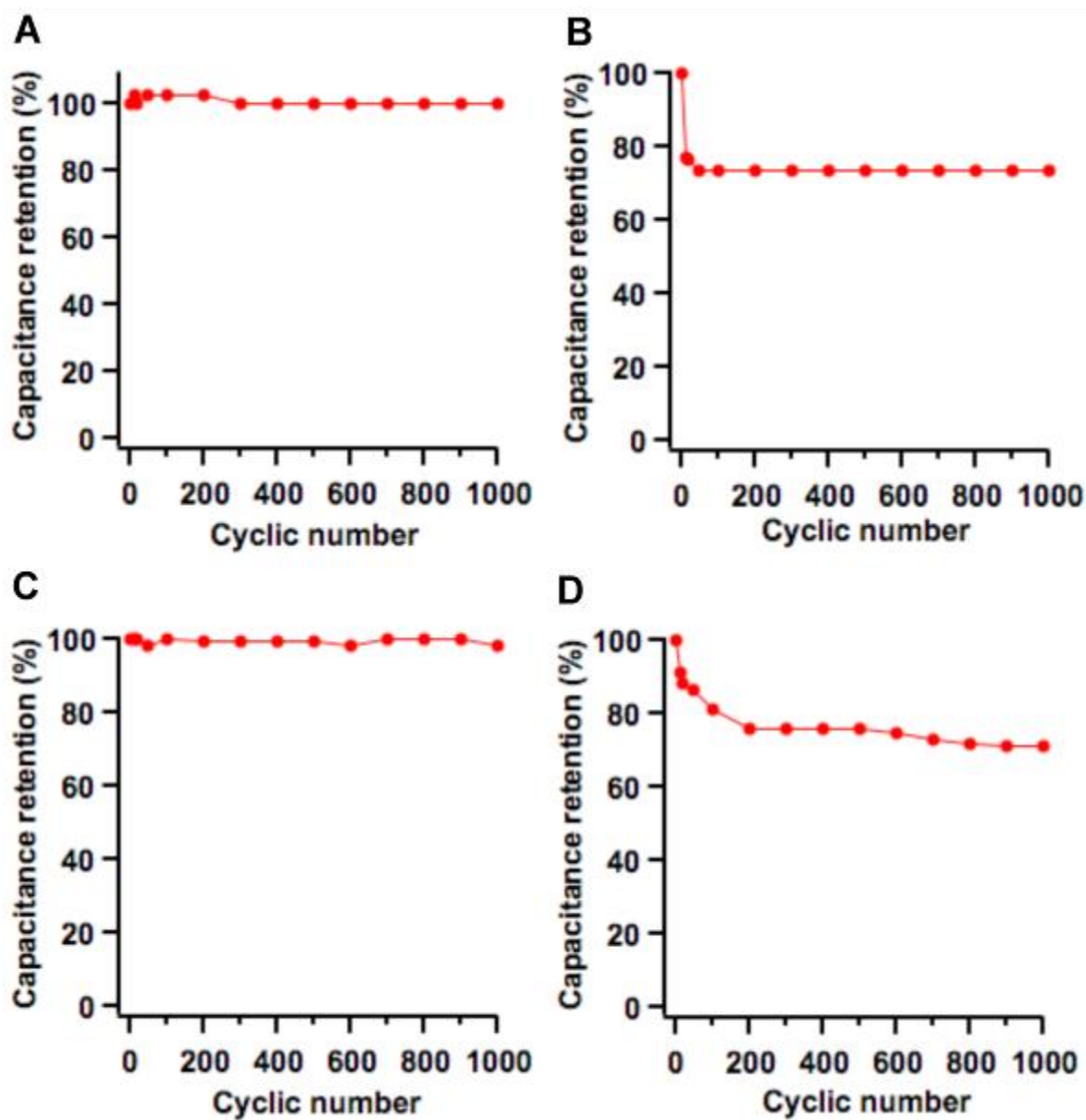


Figure S11. Cyclic stability test by charge-discharge measurements. (A) FeCP-PCP@800, (B) CoCP-PCP@800, (C) NiCP-PCP@800, (D) CuCP-PCP@800.

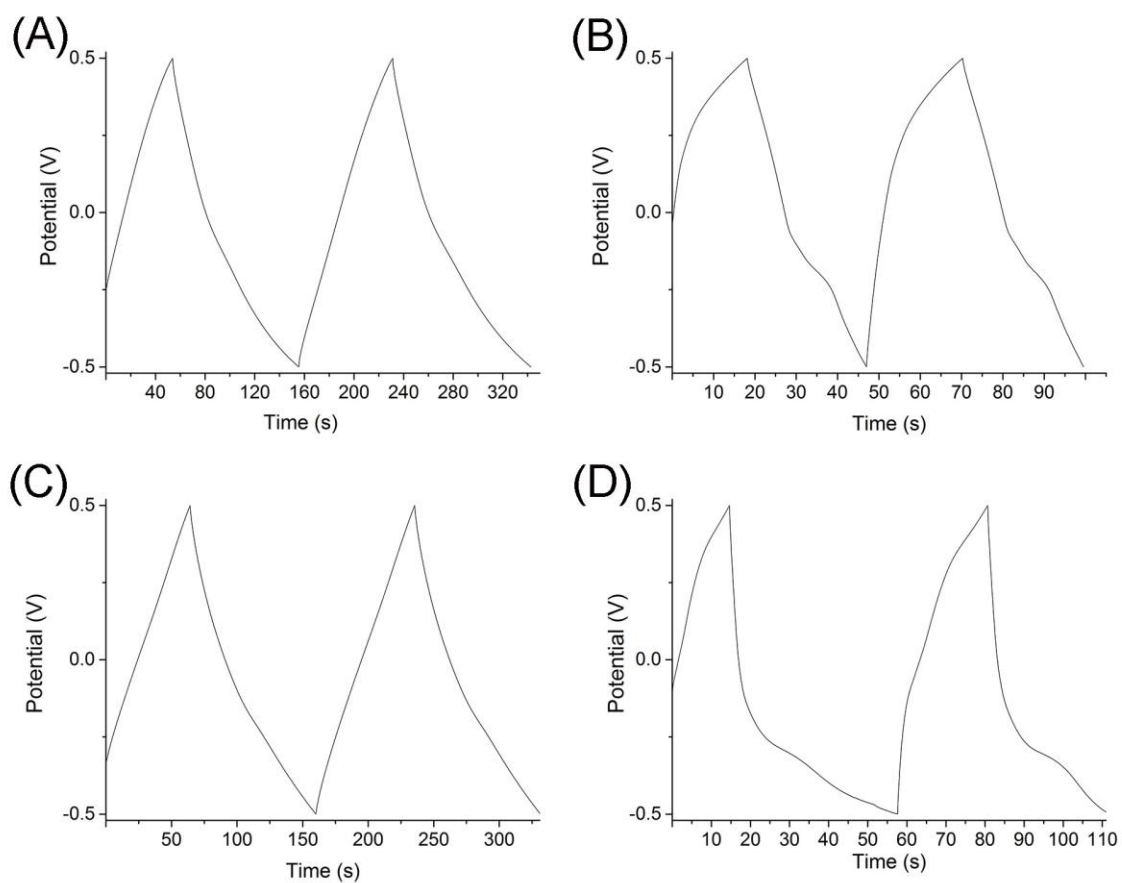


Figure S12. Charge-discharge curves at 2 A/g showing first and second cycles for (A) FeCP-PCP@800, (B) CoCP-PCP@800, (C) NiCP-PCP@800, (D) CuCP-PCP@800.

3.0 References

- S1. G. Richards and S. Swavey, *Eur. J. Inorg. Chem.* **2009**, 5367–5376.
- S2. R. P. Bonar-Law, *J. Org. Chem.* **1996**, 61, 3623–3634